ELSEVIER

www.elsevier.nl/locate/jorganchem

Journal of Organometallic Chemistry 612 (2000) 106–116

Journal of Organometallic Chemistry

Unbridged homo and hetero dinuclear complexes of Group 6 and 8 metals: synthesis, characterization and comparison of X-ray crystallographic data

Thomas Straub* [1], Matti Haukka, Tapani A. Pakkanen* [2]

Department of Chemistry, University of Joensuu, PO Box 111, FIN-80101 Joensuu, Finland

Received 12 April 2000; accepted 27 June 2000

Abstract

Several novel compounds of the type $Cp/Cp^*(CO)_3M–M'(CO)_nCp/Cp^*$ ($M = Cr$, Mo, W; $M' = Ru$, $n = 2$; $M' = Mo$, $n = 3$; $Cp = C_5H_5$, $Cp^* = C_5Me_5$) were synthesized, characterized, their structures compared and preliminary reactivity studies were carried out. The main investigations were focused on the molybdenum and ruthenium containing heterobimetallic compounds $Cp(CO)_3Mo–Ru(CO)_2Cp$ (**1**) as well as $Cp(CO)_3Mo–Ru(CO)_2Cp^*$ (**2**) and $Cp^*(CO)_3Mo–Ru(CO)_2Cp$ (**3**), the latter two representing a 'mixed-metal mixed-ligand' type of complexes with the former (**1**) having identical ligands on both metal cores. For the first time comparison of properties of unbridged bimetallic complexes with molybdenum and ruthenium metal cores was elaborated. The novel $Cp(CO)_3Mo–Mo(CO)_3Cp^*$ (**4**) consists of two identical metal cores and of 'mixed' ligands. **4** was prepared by treating $NaMo(CO)_3Cp$ with $Cp^*Mo(CO)_3Br$ (**5**) after a route for the synthesis of the latter was established. **1** reacted with halides or $AlCl_3$, respectively, under cleavage of the metal–metal bond to form $Cp(CO)_nMHal$ ($M = Mo$, $n = 3$; $M = Ru$, $n = 2$; Hal = Br, I, Cl) but was shown to be inert towards substrates such as CO_2, CO, PPh_3 or CS_2 under the chosen conditions. The corresponding anionic species $Cp(CO)_nM^-$ were obtained when **1** was reacted with alkali metal benzophenyl ketyl. © 2000 Elsevier Science B.V. All rights reserved.

Keywords: Molybdenum; Ruthenium; Crystal structures; Hetero bimetallic complexes; Carbonyl compounds

1. Introduction

Dinuclear metal complexes may be considered as cluster prototypes and may in their chemistry provide insights to reactions that occur on metal surfaces. Cyclopentadienyl molybdenum complexes of this type have been shown to be useful model systems for the basic reactions occurring in hydrodesulfurization [1] which is an important process in the refining of crude oil [2]. Since crude oil with an increasing sulfur content will be available in the future, there is particular interest in the development of new, efficient catalysts and catalyst precursors to remove the sulfur from organic compounds such as thiophene and others. Molybdenum and cobalt sulfide compounds supported on alumina are the standard catalysts for the industrial application, but there are extensive studies on the development of mixed-metal clusters that can promote the hydrodesulfurization, hydrogenation and other processes [3–5]. The major motivation is the expectation that co-operative effects between different metal atoms may promote unique patterns of substrate activation. In this respect clusters containing both molybdenum and ruthenium or more general, Group 6 and 8 metals, are of special interest due to their different properties, e.g. the oxophilicity of the former and the hydrogen activation ability of the latter. A wide range of molybdenum and ruthenium containing clusters is known and their catalytic activity is reported [3–12]. As poor to moderate yields and a lack of comprehensive systematic methods are a general drawback in cluster synthesis, we were interested in developing a general route to prepare simple heterobimetallic complexes of molybdenum and

[1] *Corresponding author. Present address: Laboratory of Organic Chemistry, Department of Chemical Technology, Helsinki University of Technology, FIN-02015 TKK, Finland. Tel.: +358-9-4515938; fax.: +358-9-4512538; e-mail: thomas.straub@hut.fi.

[2] *Corresponding author e-mail: tapani: pakkanen@joensuu.fi.

PII: S0022-328X(00)00428-9

ruthenium for the potential use as homogeneous and heterogeneous catalysts in hydrodesulfurization reactions. Furthermore they could be utilized as building blocks in the synthesis of higher clusters. Several bridged complexes of molybdenum and ruthenium are known [13–16], but only few unbridged species comprising these two metal centers have been described so far [17–20]. In this paper we present the straightforward synthesis of several novel unbridged heterobimetallic group 6-ruthenium complexes with a simple ligation prepared by metathetical reactions between $NaM(CO)_3Cp$ (M = Cr, Mo, W) and halo-ruthenium precursors [21]. The synthesis of the new homometallic 'mixed-ligand' complex $Cp(CO)_3Mo–Mo(CO)_3Cp^*$ (**4**) and reactivity studies of $Cp(CO)_3Mo–Ru(CO)_2Cp$ (**1**) are reported and the structural similarities and differences between the mixed-metal complexes $Cp(CO)_3M–Ru(CO)_2Cp$ (**1**, **6**, **7**; M = Mo, Cr, W) and the mixed-metal mixed-ligand complexes $Cp(CO)_3Mo–Ru(CO)_2Cp^*$ (**2**) and $Cp^*(CO)_3Mo–Ru(CO)_2Cp$ (**3**) are discussed in detail.

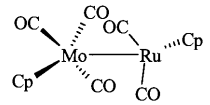

1

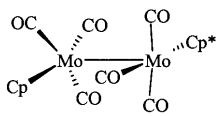

4

2. Results and discussion

2.1. Metathesis reaction of $NaM(CO)_3Cp$ (M = Cr, Mo, W) with $Ru(CO)_2CpX$ (X = Br, I)

Reaction of the anion $[Mo(CO)_3Cp]^-$ with $Ru(CO)_2CpX$ in tetrahydrofuran (THF) leads to the elimination of NaX and the formation of orange-red-crystals which were identified as the heterobimetallic complexes $Cp(CO)_3M–Ru(CO)_2Cp$ (M = Mo, Cr, W) (**1**, **6** and **7**) by IR, NMR, elemental analysis and X-ray spectroscopy. Further products formed in the reactions are the homometallic dimers $[CpRu(CO)_2]_2$ (**9**) and the corresponding $[CpM(CO)_3]_2$ (M = Cr, Mo, W) (Eq. (1)). The yields in these reactions range from 2% for **6** with the ruthenium iodide compound as the starting material and 81% for $Cp(CO)_3Mo–Ru(CO)_2Cp$ (**1**) when the ruthenium bromide complex is used. Compound **1** is also accessible by metal–metal bond metathesis between the two homometallic dimers **8** and **9** (Eq. (2)) [13,22].

$$\begin{aligned} &Na[M(CO)_3Cp] + Ru(CO)_2CpX \xrightarrow{THF,\ \Delta} \\ &\quad Cp(CO)_3M–Ru(CO)_2Cp + [Ru(CO)_2Cp]_2 \\ &\quad M = Mo\ (\mathbf{1}),\ Cr\ (\mathbf{6}),\ W(\mathbf{7}) \\ &\quad + [M(CO)_3Cp]_2 \\ &\qquad M = Cr,\ Mo,\ W \end{aligned} \tag{1}$$

$$\begin{aligned} &[Mo(CO)_3Cp]_2 + [Ru(CO)_2Cp]_2 \xrightarrow{Tol,\ \Delta} \\ &\quad \mathbf{8} \qquad\qquad \mathbf{9} \\ &\quad Cp(CO)_3M–Ru(CO)_2Cp \\ &\qquad\quad \mathbf{1} \end{aligned} \tag{2}$$

2.2. Synthesis of $Cp(CO)_3Mo–Ru(CO)_2Cp^*$ (2), $Cp^*(CO)_3Mo–Ru(CO)_2Cp$ (3), $Cp(CO)_3Mo–Mo(CO)_3Cp^*$ (4) and $Cp^*(CO)_3MoBr$ (5)

The mixed-ligand complexes **2**, **3** and **4** were synthesized by treating the sodium metallates with the appropriate bromide complex. It is noteworthy that the reactions failed when the corresponding iodides were used, a phenomenon that is also observed in the preparation of $Cp(CO)_2Fe–Fe(CO)_2Cp^*$ [23]. In all cases only the formation of the corresponding homometallic dimers bearing either Cp or Cp* was obtained exclusively. Given this, a route for the synthesis of $Cp^*(CO)_3MoBr$ (**5**) had to be elaborated. Compound **5** is mentioned in the literature to be formed from the bromomethyl metal complex $Cp^*(CO)_3MoCH_2Br$ under reflux in methanol [24], but no synthesis or analytical data were available to date. While treatment of $[Cp^*Mo(CO)_3]_2$ (**13**) with the dihalogen I_2 yields $Cp^*(CO)_3MoI$ [25], **5** cannot be obtained in a similar way due to further oxidation of the possibly initially formed target compound even when **13** is used in excess [26,27]. The method of choice was a modified reaction sequence used for the synthesis of $Cp(CO)_3MoI$ [28]. At 0°C the carbonyl metallate $NaMo(CO)_3Cp$ [29] was oxidized with Br_2 to yield **5** quantitatively. At higher temperatures initially formed **5** reacts with the not yet consumed $NaMo(CO)_3Cp$ to form the dimer **13** which is subsequently oxidized by Br_2 under multiple bromination.

2.3. Preliminary reactivity studies of $Cp(CO)_3Mo–Ru(CO)_2Cp$ (1)

The reactivity of **1** was tested with several substrates (Scheme 1) and the reactions monitored by IR spectroscopy. The reported products were not isolated. **1** is stable under reflux in THF for 3 days and thermal activation of the molecule did not lead to reaction with PPh_3 or CS_2, respectively. In this context we tried unsuccessfully to synthesize $Cp(CO)_3Mo–Ru(CO)_3(\eta^3\text{-}C_3H_5)$ (**14**) with a supposedly higher potential for carbonyl replacement, but no complex bearing an allyl ligand was accessible. Reaction of **1** with $AlCl_3$ or

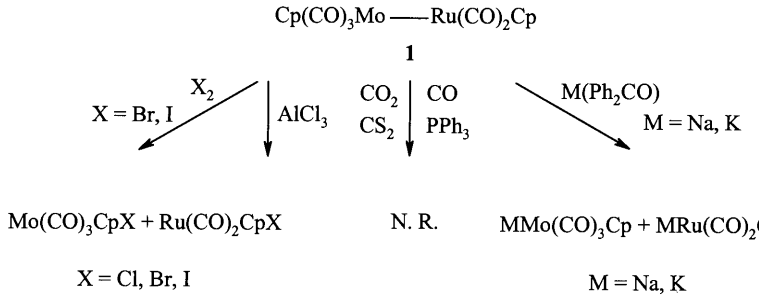

Scheme 1. Reactivity of $Cp(CO)_3Mo–Ru(CO)_2Cp$ (**1**).

solutions of Br_2 or I_2 in THF leads to a metal–metal bond cleavage and to the expected formation of the molybdenum and ruthenium halides. The corresponding molybdates and ruthenates are obtained when **1** is treated with THF solutions of $Na(Ph_2CO)$ or $K(Ph_2CO)$ and no further reduction was detected upon addition of excess $Na(Ph_2CO)$ or $K(Ph_2CO)$. Furthermore, no reaction was detected with carbon monoxide or carbon dioxide.

2.4. X-ray crystallographic analysis

The molecular configurations of **1** and **2** are shown in Figs. 1 and 2, and details of selected bond lengths and

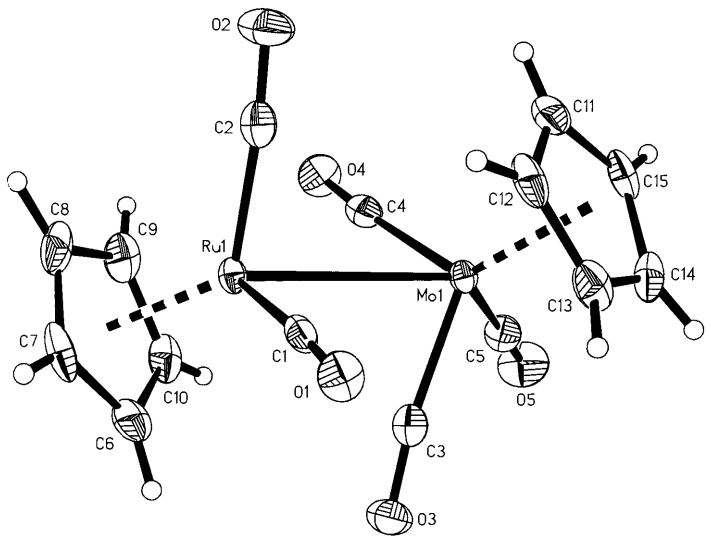

Fig. 1. ORTEP plot of $Cp(CO)_3Mo–Ru(CO)_2Cp$ (**1**) with ellipsoids drawn in 50% probability.

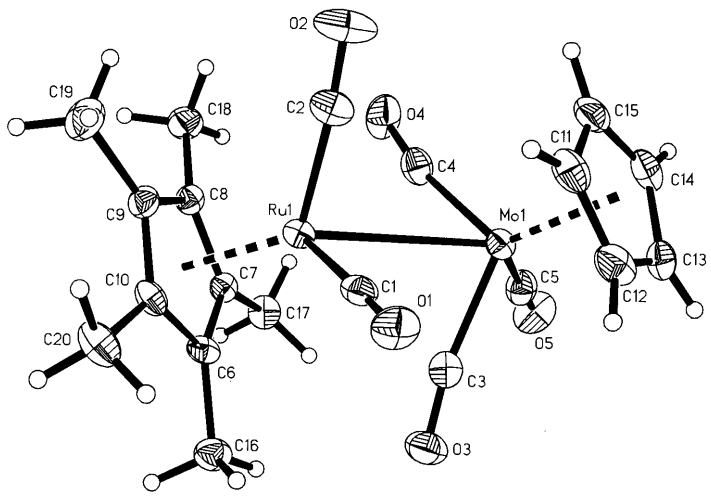

Fig. 2. ORTEP plot of $Cp(CO)_3Mo–Ru(CO)_2Cp^*$ (**2**) with ellipsoids drawn in 50% probability.

Table 1
Crystallographic data for $Cp(CO)_3Mo–Ru(CO)_2Cp$ (**1**), $Cp(CO)_3Mo–Ru(CO)_2Cp^*$ (**2**), $Cp(CO)_3Cr–Ru(CO)_2Cp$ (**6**) and $Cp(CO)_3W–Ru(CO)_2Cp$ (**7**)

	1	**2**	**6**	**7**
Empirical formula	$C_{15}H_{10}MoO_5Ru$	$C_{20}H_{20}MoO_5Ru$	$C_{15}H_{10}CrO_5Ru$	$C_{15}H_{10}O_5RuW$
Molecular weight	467.24	537.37	423.30	555.15
Crystal size (mm)	$0.20\times0.20\times0.05$	$0.30\times0.30\times0.20$	$0.50\times0.20\times0.10$	$0.30\times0.30\times0.10$
Crystal system	Monoclinic	Monoclinic	Monoclinic	Monoclinic
Space group	$P2_1/n$	$P2_1/n$	$P2_1/c$	$P2_1/c$
λ (Å)	0.71073	0.71073	0.71073	0.71073
Unit cell dimensions				
a (Å)	8.3175(2)	9.6745(2)	9.2976(3)	9.5378(2)
b (Å)	11.1579(2)	26.4386(4)	11.5439(2)	11.5926(2)
c (Å)	16.3715(4)	15.7341(3)	14.0692(4)	14.1015(2)
β (°)	102.540(1)	100.8910(10)	99.5310(10)	101.700(1)
V (Å^3)	1483.13(6)	3951.98(13)	1489.21(7)	1526.78(5)
Z	4	8	4	4
D_{calc} (g cm^{-3})	2.093	1.806	1.888	2.415
μ (mm^{-1})	1.883	1.426	1.762	8.536
T (K)	120(2)	120(2)	120(2)	120(2)
θ Range (°)	3.65–26.37	1.53–27.46	3.81–27.47	3.81–25.00
No. of unique reflections	3019	8803	3210	2677
No. of observed data [a]	2619	7287	2869	2630
No. of parameters	239	497	240	199
R_1	0.0221	0.0268	0.0238	0.0193
wR^2	0.0480	0.0506	0.0598	0.0487
Largest difference peak and hole (e Å^{-3})	0.485 and −0.609	0.432 and −0.546	0.8435 and 0.4728	1.200 and −1.089

[a] $I>2\sigma$.

angles for **1**, **2**, **6**, **7** and **9** are given in Table 2. The complexes **1**, **6** and **7** consist of $M(CO)_3Cp$ (M = Mo, Cr, W) and $Ru(CO)_2Cp$ fragments linked by an unsupported Ru–M bond. In **2** the Cp ligand is replaced by a Cp* moiety, but otherwise the bonding situation is similar to **1**. **2** crystallizes in an asymmetric unit, but one molecule can be neglected for the discussion. The details are given in Section 5.

The five carbonyl ligands in **1**, **2**, **6** and **7** are all terminal, reflected by M(1)–M(2)–CO angles not smaller than 65° and M–C–O angles larger than 168.7°. However, comparison of **1** and **2** shows that there is a tendency towards smaller angles for the complex bearing the Cp* ligand. In **2** the Mo(1)–C(3)–O(3) and Mo(1)–C(4)–O(4) angles decrease by 2.5 and 3.5°, respectively, while the Mo(1)–C(5)–O(5) and Ru(1)–C–O angles remain virtually unchanged. Since also the M–M–C(1–5) angles decrease by a maximum of 4.5° and the change is more pronounced for the molybdenum fragment, one has to argue that this stronger 'bending' of the carbonyl ligands towards the other metal fragment is a result of the new electronic situation with a higher electron density rather than of change in steric requirements which should have the opposite effect. The Cp/Cp or Cp/Cp* ligands of all the novel complexes adopt a centric coordination to the metals and are found in *trans* position relative to the M–Ru vector. Furthermore the Cp and Cp* moieties exhibit structural properties known from related compounds [17,30–32]. The M–Ru bond lengths of 2.9435(6) for **6** and 3.0101(3) Å for **1** lie in the metal–ruthenium single bond range. As expected, they are 0.04–0.05 Å longer than the corresponding bonds in their iron homologues where 2.901(1) and 2.963(1) Å are found for the Fe–Cr [30] bond and the Fe–Mo [31] bond, respectively. Compound **1** displays a Mo–Ru bond length 0.05 Å longer than the corresponding one in $(\eta^7\text{-}C_7H_7)(CO)_2Mo–Ru(CO)_2Cp$ [17], which is attributed to higher number of carbonyl ligands. In **2** the metal–metal bond is determined to be 3.0424(3) Å, constituting an elongation of the Mo–Ru in comparison to **1**. Similar observations are made for bimetallic complexes when Cp is replaced by Cp* [32,33]. The $M(CO)_3Cp$ fragments essentially adopt a piano-stool geometry and a mirror plane through both metal cores and the Cp or Cp* centroids is inherent in the complexes. While **2** is almost perfect in plane, the other compounds are also only slightly distorted from it.

2.5. Spectroscopic results

The pattern of the IR absorptions for **1**, **6** and **7** compares with that of the corresponding iron homologues [22,31] suggesting a similar structure. The most significant feature in the IR spectra is the absence of bands that indicate bridging carbonyl ligands, suggesting an all-terminal carbonyl structure featuring an unbridged metal–metal bond (Table 3).

In contrast to the iron homologues, for the ruthenium complexes additional weak absorptions are observed that add up to more bands than carbonyl ligands. For the five carbonyl groups of **1** up to seven IR-bands are detected depending on the solvent. Therefore the presence of isomers has to be assumed [22]. Besides the main *trans*-isomer, *cis* or anti and gauche [34] conformers might be formulated. However, there is no indication of isomeric forms comprising bridging carbonyl ligands. The 'mixed-metal mixed-ligand' compounds **2** and **3** show surprisingly different IR spectra (Fig. 3).

Compared with **1**, the bands of **2** and **3** show a red shift, which reflects a higher electron density around the metals [35]. While with basically three bands the IR patterns for both compounds in THF are essentially the same, the situation changes in hexane. For **2** the pattern is almost identical with that for complex **1** while for **3** the three-absorption pattern is basically retained. The only chemical difference between **1**, **2** and **3** is the change of a Cp to a Cp* and the position of this ligand in the molecule. So, one can reason that the relatively large steric requirements of the Cp* in conjunction with the metal carbonyl fragment to which it is bound to may prevent rotation around the metal–metal bond. Consequently one can argue that the sterically more demanding $Mo(CO)_3Cp^*$ fragment in **3** promotes the *trans* form that is also found in the solid state, while in **2** with the smaller $Ru(CO)_2Cp^*$ moiety the formation of conformers is still possible [17]. The IR spectra of $Cp(CO)_3Mo–Mo(CO)_3Cp^*$ (**4**) compares nicely with the spectra of $Cp(CO)_3Mo–Mo(CO)_3Cp$ (**8**) and $Cp^*(CO)_3Mo–Mo(CO)_3Cp^*$ (**13**), retaining the basic absorption pattern invoked by the same structural family of complexes and approximately averaging out the wave numbers reflecting the new electronic situation.

Table 2
Selected bond distances (Å) and bond angles (°) for $Cp(CO)_3Mo–Ru(CO)_2Cp$ (**1**), $Cp(CO)_3Mo–Ru(CO)_2Cp^*$ (**2**) $Cp(CO)_3Cr–Ru(CO)_2Cp$ (**6**), $Cp(CO)_3W–Ru(CO)_2Cp$ (**7**) and $Cp(CO)_2Ru–Ru(CO)_2Cp$ (**9**) [a]

	1	**2**	**6**	**7**	**9**
Ru(1)–M(1)	3.0101(3)	3.0424(3)	2.9435(6)	2.9974(3)	2.7412(4)
Ru(1)–C(1)	1.871(3)	1.874(3)	1.874(3)	1.865(4)	1.862(3)
Ru(1)–C(2)	1.869(3)	1.863(3)	1.876(3)	1.866(4)	2.037(3)
Ru(1) # –C(2)					2.040(3)
Ru(1)–C(6)	2.254(3)	2.270(2)	2.256(3)	2.262(4)	2.280(3)
Ru(1)–C(7)	2.227(3)	2.299(2)	2.230(3)	2.237(4)	2.297(3)
Ru(1)–C(8)	2.233(3)	2.270(2)	2.232(3)	2.244(4)	2.257(3)
Ru(1)–C(9)	2.253(3)	2.230(3)	2.255(3)	2.265(4)	2.234(2)
Ru(1)–C(10)	2.269(3)	2.235(2)	2.279(3)	2.283(4)	2.280(3)
M(1)–C(3)	1.968(3)	1.973(3)	1.852(3)	1.968(4)	
M(1)–C(4)	1.980(3)	1.970(3)	1.831(3)	1.977(4)	
M(1)–C(5)	1.960(3)	1.944(3)	1.854(3)	1.963(4)	
M(1)–C(11)	2.347(3)	2.394(3)	2.241(3)	2.314(4)	
M(1)–C(12)	2.398(3)	2.361(3)	2.211(3)	2.363(4)	
M(1)–C(13)	2.356(3)	2.314(3)	2.172(3)	2.397(4)	
M(1)–C(14)	2.312(3)	2.325(3)	2.177(3)	2.362(4)	
M(1)–C(15)	2.320(3)	2.369(3)	2.218(3)	2.317(4)	
Ru(1)–C(1)–O(1)	175.8(2)	176.6(2)	178.7(2)	176.8(3)	178.8(2)
Ru(1)–C(2)–O(2)	175.0(3)	174.8(3)	176.6(2)	178.4(4)	138.2(2)
Ru(1) # –C(2)–O(2)					137.3(2)
M(1)–C(3)–O(3)	172.9(2)	170.4(2)	170.5(2)	173.5(3)	
M(1)–C(4)–O(4)	172.2(2)	168.7(2)	172.1(2)	173.9(3)	
M(1)–C(5)–O(5)	179.1(3)	178.0(2)	179.3(3)	179.0(3)	
Ru(1)–M(1)–C(3)	70.36(8)	68.67(8)	65.01(8)	70.36(8)	
Ru(1)–M(1)–C(4)	68.63(8)	65.37(8)	69.04(8)	68.63(8)	
Ru(1)–M(1)–C(5)	126.58(8)	122.09(8)	119.72(9)	126.58(8)	
M(1)–Ru(1)–C(1)	82.82(8)	79.39(8)	84.15(8)	82.82(8)	93.09(8)
M(1)–Ru(1)–C(2)	85.94(8)	84.82(9)	84.06(7)	85.94(8)	47.79(7)
M(1)–Ru(1)–C(2) #					47.71(7)
C(1)–Ru(1)–Mo(1)–C(3)	72.61(11)	71.59(11)	68.05(12)	77.36(17)	
C(1)–Ru(1)–Mo(1)–C(4)	−173.05(11)	−164.25(12)	−163.16(11)	−162.36(17)	
C(1)–Ru(1)–Mo(1)–C(5)	130.81(12)	134.28(12)	130.21(12)	138.37(18)	
C(2)–Ru(1)–Mo(1)–C(3)	165.34(11)	163.30(12)	159.25(12)	169.28(16)	
C(2)–Ru(1)–Mo(1)–C(4)	−80.32(12)	−72.54(12)	−71.96(12)	−70.44(17)	
C(2)–Ru(1)–Mo(1)–C(5)	−136.46(13)	−134.01(13)	−138.59(12)	−129.71(18)	

[a] M = Cr, Mo, W, Ru.

Table 3
IR data [a]

Complex	ν(CO) (cm^{-1})
1	2020 (vw), 2008 (vw), 1965 (vs), 1953 (vs), 1921 (vw), 1902 (w), 1888 (m) [b]
	2022 (vw), 2007 (vw), 1963 (vs), 1953 (vs), 1919 (vw), 1900 (w), 1887 (m) [c]
	2015 (vw), 2004 (vw), 1954 (vs), 1912 (vw), 1877 (m, br) [d]
	2017 (vw), 2004 (vw), 1955 (vs), 1948 (vs), 1912 (vw), 1890 (sh), 1876 (m) [e]
	2012 (sh), 2007 (vw), 1954 (vs), 1875 (m, br) [f]
2	1996 (vw), 1950 (vs), 1944 (vs), 1913 (vw), 1885 (vw), 1870 (w) [b]
	1993 (vw), 1940 (vs), 1862 (m, br) [d]
3	2000 (vw), 1947 (vs), 1909 (vw), 1880 (m) [b]
	1995 (vw), 1940 (vs), 1869 (m, br) [d]
4	1951 (vs), 1913 (s), 1897 (w) [b]
	2003 (vw), 1945 (vs), 1907 (s), 1889 (m) [d]
5	2039 (s), 1967 (vs), 1940 (s) [d]
6	2024 (vw), 2012 (w), 1962 (vs), 1950 (vs), 1912 (vw), 1890 (w), 1877 (m) [b]
7	2020 (vw), 2006 (vw), 1963 (vs), 1951 (s), 1913 (vw), 1896 (w), 1883 (m) [b]
8	2011 (w), 1956 (vs), 1912 (s) [d]
13	1932 (vs), 1989 (m, br) [d]

[a] w = weak, vw = very weak, m = medium, s = strong, vs = very strong, sh = shoulder, br = broad.
[b] In hexane.
[c] In cyclohexane.
[d] In THF.
[e] In toluene.
[f] In CH_2Cl_2.

The proton NMR spectra of **1**, **6** and **7** show two signals in a 1:1 ratio for the Cp ligands. An unambiguous assignment to the metal centers is possible by comparing the chemical shifts to related compounds [17,22] and the complexes **2** and **3**. The latter two exhibit two signals of an intensity of 3:1 which reflect a Cp* and a Cp ligand, respectively. A comparison of the proton NMR data of the molybdenum and/or ruthenium containing complexes **1**–**4**, **8**, **9** and **13** reveals the trend to a relative high field shift for the ruthenium fragments, whereas molybdenum moieties are shifted to lower field in the mixed metal complexes. This is in agreement with the finding that in heterobimetallic complexes a metal fragment usually shows a high field shift when the introduced other metal fragment bears carbonyl ligands exclusively and that the opposite effect is observed for the introduction of fragments with a Cp ligand [22]. In the mixed metal complexes reported in this paper the relative number of carbonyl ligands in $Mo(CO)_3Cp/Cp^*$ and $Ru(CO)_2Cp/Cp^*$ is arguably responsible for the observed trend. The nature of the Cp/Cp* ligand does not contribute to it significantly, as derived from the proton NMR data of **4**, where the shift of the two signals is only -0.02 ppm and $+0.02$ ppm relative to the corresponding complexes **8** and **13**. For none of the compounds signals indicating isomers were observed, which excludes an intermetallic Cp/Cp* exchange. Due to the tendency of **6** to homolytic cleavage of the metal–metal bond and formation of the homometallic dimers and $Cp(CO)_3Cr\cdot$ [36] it proofed impossible to obtain a pure analytical sample or a satisfying NMR of the complex. Due to the presence of small concentrations of the paramagnetic $Cp(CO)_3Cr\cdot$ usually no signal could be detected in the NMR spectra, with only one exception, where **6** was contaminated with minor amounts of $[CpRu(CO)_2]_2$ (**9**).

In the carbon NMR spectra, the most prominent common feature for all the mixed metal complexes as well as the homometallic mixed-ligand complex **4** is the single resonance for the carbonyl groups at room temperature which indicates a facile and rapid interchange of all the carbonyl groups of the molecule in and between the two metal moieties in solution. The proposed structures are confirmed by the observed additional resonances. Two doublets around 90 ppm, characteristic for Cp ligands, are detected for **1** and **7**. The carbon NMR spectra of the mixed-ligand complexes **2**, **3** and **4** exhibit a doublet in the same region for the Cp and a quartet for the methyl groups as well as a singlet for the quaternary carbon of the Cp* ligand.

3. Conclusions

We have successfully demonstrated that the metathesis reaction between $NaM(CO)_3Cp/Cp^*$ (M = Cr, Mo, W) with $Ru(CO)_2Cp/Cp^*X$ (X = Br, I) or $Mo(CO)_3Cp^*Br$ is a powerful tool for the synthesis of unbridged homobimetallic and heterobimetallic complexes of Group 6 metals and ruthenium. For the molybdenum–ruthenium complexes ligand variation was feasible, giving rise to the complexes **1**, **2** and **3** which reveal intriguing structural similarities and differences. For the first time comparison of properties of unbridged bimetallic complexes with molybdenum and ruthenium metal cores was elaborated. Preliminary reactivity studies on **1** reveal that carbonyl displacement is not favored and that reactions occur under cleavage of the metal–metal bond. Further investigations concerning reactivity and catalytic activity of molybdenum–ruthenium compounds are underway.

4. Experimental

4.1. Materials and methods

All manipulations of air-sensitive materials were performed under a nitrogen atmosphere in conventional Schlenk apparatus. Solvents were distilled from Na/K

or Na benzophenyl ketyl under nitrogen. Hexane for column chromatography was deoxygenated but otherwise used as received. Deuterated solvents were deoxygenated (three freeze–pump–thaw cycles) and stored under nitrogen over molecular sieves. Cyclopentadienyl sodium, pentamethyl-cyclopentadienyl sodium, allyl bromide, $M(CO)_6$ (M = Cr, Mo, W), $[Mo(CO)_3Cp]_2$ (**8**) (all purchased from Aldrich) and $[Ru(CO)_3Cl_2]_2$ (Johnson and Matthey) were used as received. Silica gel 60 (0.063–0.200 mm, Merck) for column chromatography was kept under HV for 5 h and saturated with nitrogen before use. Column properties: 2 × 20 cm (if not stated otherwise), mobile phase at start: hexane. Volume of reaction mixtures loaded onto the column: max. 2 ml in THF.

$NaM(CO)_3Cp$ (M = Cr, Mo, W) [29], $NaMo(CO)_3$-Cp* [29], $CpMo(CO)_3$] [37], $[CpRu(CO)_2]_2$ (**9**) [37], $[Cp^*Ru(CO)_2]_2$ (**10**) [38], $CpRu(CO)_2X$ (X = Br, I) [39], $Cp^*Ru(CO)_2X$ (X = Br, I) [25] and (η^3-C_3H_5)Ru-$(CO)_3Br$ (**11**) [40] were prepared according to methods reported in the literature.

Infrared spectra were measured on a Nicolet Magna 705 FTIR spectrometer in hexane or THF solution, respectively. ^{1}H- and ^{13}C-NMR spectra were recorded on a Bruker Avance 250 MHz spectrometer using C_6D_6 (if not stated otherwise) as solvent. Chemical shifts for ^{1}H- and ^{13}C-NMR are referenced to internal solvent resonances and are reported relative to tetramethylsilane ($\delta = 7.15$ ppm and 127 ppm, respectively, for C_6D_6). Elemental analysis were performed with an EA1110 CHNS–O analyzer (Carlo Erba instruments).

4.2. $Cp(CO)_3Mo–Ru(CO)_2Cp$ (*1*)

At room temperature (r.t.), a solution of 604 mg (2.0 mmol) $CpRu(CO)_2Br$ in 20 ml THF was added dropwise to 536 mg (2.0 mmol) $NaMo(CO)_3Cp$ in 20 ml THF. After 6 h of refluxing the reaction was terminated, the mixture concentrated and separated into its components. Fraction 1 (eluent: hexane–THF 25:1): 563 mg (1.2 mmol, 60%) orange needles of $Cp(CO)_3Mo–Ru(CO)_2Cp$ (**1**) (from hexane at −25°C, crystals suitable for X-ray crystallography). ^{1}H-NMR (ppm): 4.84 (s, 5H, MoCp), 4.57 (s, 5H, RuCp). ^{13}C-NMR (ppm): 219.5 (s, CO), 89.7 (d, $^1J_{CH} = 177$ Hz, MoCp), 87.5 (d, $^1J_{CH} = 177$ Hz, RuCp). Anal. Calc. for $C_{15}H_{10}O_5MoRu$ (FW = 467.25): C, 38.56; H, 2.16. Found: C, 38.94; H, 2.15%. Fraction 2 (hexane–THF 10:1): 190 mg (0.4 mmol, 21%) (**1**), after crystallization from small amounts of $[CpRu(CO)_2]_2$ (**9**) (hexane, −25°C). Fraction 3 (THF): traces of $CpRu(CO)_2Br$, (**1**),

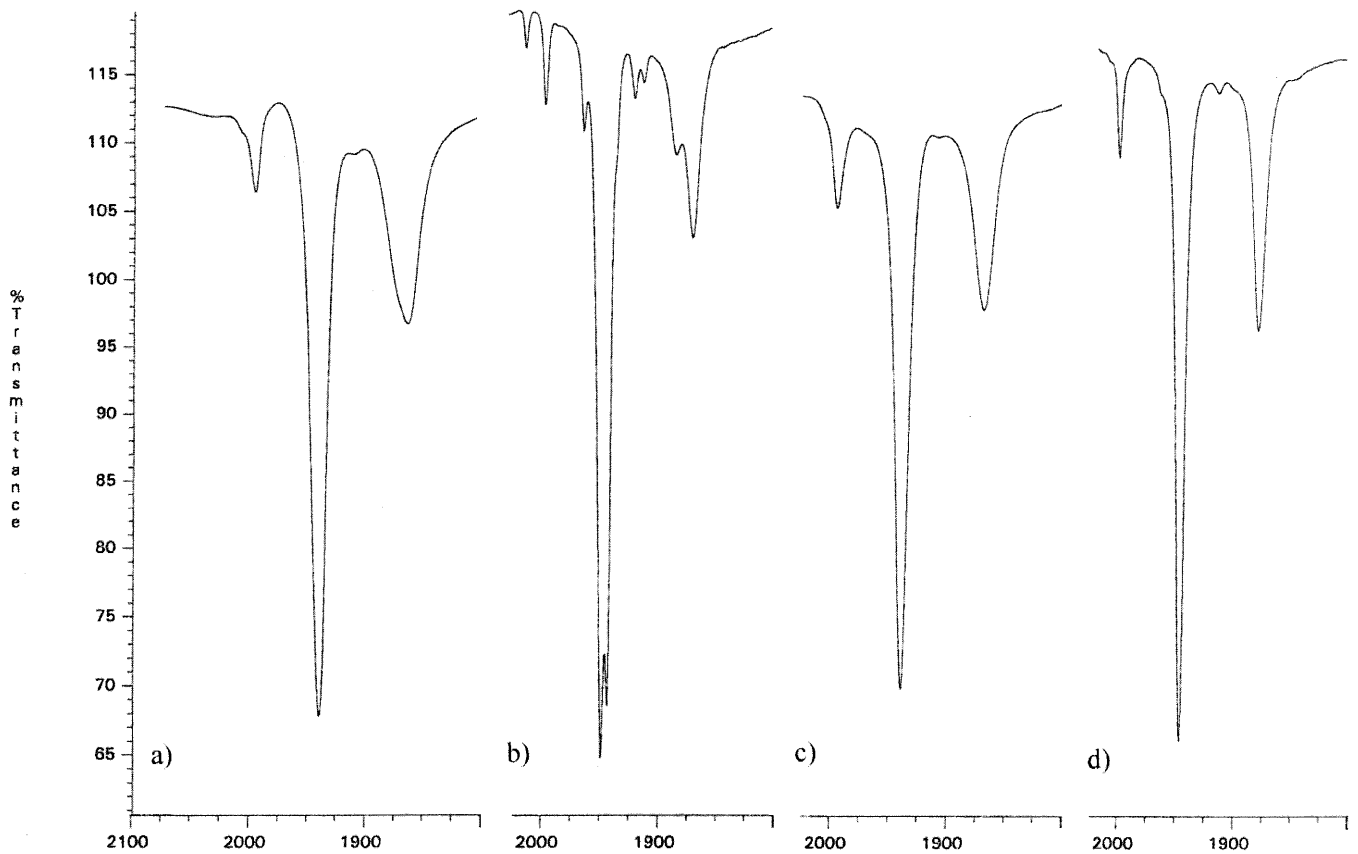

Fig. 3. IR-spectra of $Cp(CO)_3Mo–Ru(CO)_2Cp^*$ (**2**): (a) in THF; (b) in hexane and of $Cp^*(CO)_3Mo–Ru(CO)_2Cp$ (**3**); (c) in THF; (d) in hexane.

$[CpMo(CO)_3]_2$ (**8**), discarded. When $Cp(CO)_2RuI$ was used instead of $CpRu(CO)_2Br$ the reaction time increased (up to 4 days), the yield decreased (max. 67%), and the reaction did not go to completion. **1** was also isolated in 15% yield from the thermal reaction of $[CpMo(CO)_3]_2$ (**8**) and $[CpRu(CO)_2]_2$ (**9**) in toluene.

4.3. $Cp(CO)_3Mo–Ru(CO)_2Cp^*$ (2)

As described above, a solution of 372 mg (1.0 mmol) $Cp^*Ru(CO)_2Br$ in 20 ml THF was added dropwise to 532 mg (2.0 mmol) $NaMo(CO)_3Cp$ in 20 ml THF. After 8 days of refluxing the $Cp^*Ru(CO)_2Br$ is consumed. The mixture was concentrated and separated into its components. Fraction 1 (hexane–THF 25:1, followed by extraction with hexane): 168 mg (0.31 mmol, 31%) orange crystals of $Cp(CO)_3Mo–Ru(CO)_2Cp^*$ (**2**) (from hexane at +5°C, crystals suitable for X-ray crystallography). ^{1}H-NMR (ppm): 4.91 (s, 5H, Cp), 1.62 s, 15H, Cp*). ^{13}C-NMR (ppm): 221.7 (s, CO), 99.3 (s, Cp*), 89.7 (d, $^1J_{CH} = 176$ Hz, Cp), 8.9 (q, $^1J_{CH} = 128$ Hz, Cp*). Anal. Calc. for $C_{20}H_{20}O_5MoRu$ (FW = 537.38): C, 44.70; H, 3.75. Found: C, 44.70; H, 3.78%. No further fractions were collected.

4.4. $Cp^*(CO)_3Mo–Ru(CO)_2Cp$ (3)

As described above, a solution of 967 mg (3.2 mmol) $CpRu(CO)_2Br$ in 20 ml THF was added dropwise to 1082 mg (3.2 mmol) $NaMo(CO)_3Cp^*$ in 20 ml THF. After 2 h of stirring at r.t. and another 2 h reflux, the reaction was complete. The mixture was stirred over night under a CO atmosphere (conversion of $[Cp^*Mo(CO)_2]_2$ (**12**) to $[Cp^*Mo(CO)_3]_2$ (**13**) and therefore easier purification of the desired product), then concentrated and separated into its components. Fraction 1 (hexane–THF 25:1): 705 mg (1.3 mmol, 41%) red–orange needles of $Cp^*(CO)_3Mo–Ru(CO)_2Cp$ (**3**) (from hexane at −25°C). ^{1}H-NMR (ppm): 4.61 (s, 5H, Cp), 1.84 s, 15H, Cp*). ^{13}C-NMR (ppm): 224.0 (s, CO), 103.2 (s, Cp*), 87.6 (d, $^1J_{CH} = 179$ Hz, Cp), 9.9 (q, $^1J_{CH} = 128$ Hz, Cp*). Anal. Calc. for $C_{20}H_{20}O_5MoRu$ (FW = 537.38): C, 44.70; H, 3.75. Found: C, 44.83; H, 3.81%. Fraction 2 (hexane–THF 10:1): 228 mg (0.57 mmol, 18%) (**5**). No further fractions were collected.

4.5. $Cp(CO)_3Mo–Mo(CO)_3Cp^*$ (4)

At −78°C, a solution of 780 mg (2.0 mmol) $Cp^*Mo(CO)_3Br$ (**5**) in 20 ml THF was added dropwise to 536 mg (2.0 mmol) $NaMo(CO)_3Cp$ in 20 ml THF. The reaction mixture is allowed to warm to r.t. and stirred for 8 h. After 1 h of refluxing the mixture was concentrated and separated into its components. Fraction 1 (hexane–THF 50:1): 482 mg (0.86 mmol, 43%) dark red crystals of $Cp(CO)_3Mo–Mo(CO)_3Cp^*$ (**4**) (from hexane–THF at −25°C). ^{1}H-NMR (ppm): 4.68 (s, 5H, Cp), 1.73 s, 15H, Cp*). ^{13}C-NMR (ppm): 231.7 (s, CO), 104.7 (s, Cp*), 90.6 (d, $^1J_{CH} = 178$ Hz, Cp), 9.7 (q, $^1J_{CH} = 128$ Hz, Cp*). Anal. Calc. for $C_{21}H_{20}O_6Mo_2$ (FW = 560.26): C, 45.02; H, 3.60. Found: C, 45.22; H, 3.68%. Fraction 2 (hexane–THF 10:1): $[CpMo(CO)_3]_2$ (**8**).

Interestingly, only $[CpMo(CO)_3]_2$ (**8**), $[Cp^*Mo(CO)_3]_2$ (**13**) and the halides $CpMo(CO)_3I$ and $Cp^*Mo(CO)_3I$ were isolated when $CpMo(CO)_3I$ was used as a starting material. At −78°C, 744 mg (2.0 mmol) of $CpMo(CO)_3I$ in 20 ml THF were added to a solution of 676 mg (2.0 mmol) $NaMo(CO)_3Cp^*$ in 20 ml THF. $NaMo(CO)_3Cp$ and $Cp^*Mo(CO)_3I$ were formed spontaneously. It was allowed to warm to r.t., refluxed for 2 days and stirred under CO atmosphere for 16 h. Column chromatography lead to the pure compounds **8**, **13**, $CpMo(CO)_3I$ and $Mo(CO_3)Cp^*I$. Spectroscopic data of $Mo(CO_3)Cp^*I$: IR (hexane) (cm^{-1}): 2030 (vs), 1962 (vs), 1939 (s). ^{1}H-NMR (ppm): 1.58 (s). ^{13}C-NMR (ppm): 241.3 (s, CO *trans*), 223.6 (s, CO *cis*), 106.2 (Cp*), 9.9 (q, $^1J_{CH} = 128$ Hz, Cp*).

4.6. $Mo(CO)_3Cp^*Br$ (5)

At 0°C, 676 mg (2.0 mmol) of $NaMo(CO)_3Cp^*$ in 20 ml THF are treated with a solution of bromine in THF. The reaction is monitored by IR and terminated after all the starting material is consumed. The reaction mixture is filtered, concentrated and the product purified by column chromatography. **5** is eluted as a red band with THF. 650 mg (1.65 mmol, 83%) orange–red crystals. ^{1}H-NMR (ppm): 1.46 (s). ^{13}C-NMR (ppm): 244.3 (s, CO *trans*), 225.2 (s, CO *cis*), 106.9 (Cp*), 9.4 (q, $^1J_{CH} = 128$ Hz, Cp*). Anal. Calc. for $C_{13}H_{15}BrO_3Mo$ (FW = 395.10): C, 39.52; H, 3.83. Found: C, 39.66; H, 3.84%. For further reactions with metal organyls **5** was usually used in situ without further purification.

4.7. $Cp(CO)_3Cr–Ru(CO)_2Cp$ (6)

A solution of 604 mg (2.0 mmol) $CpRu(CO)_2Br$ in 15 ml THF was added dropwise to 448 mg (2.0 mmol) $NaCr(CO)_3Cp$ in 15 ml THF. It was refluxed for 48 h and worked up as described above. In addition several crystallizations were performed. Fraction 1 (hexane–THF 10:1): yield $\ll 1\%$, red crystals of $Cp(CO)_3Cr–Ru(CO)_2Cp$ (**6**) (from hexane at −25°C, crystals suitable for X-ray crystallography). ^{1}H-NMR (ppm): 4.51 (s, 5H, Cp), 4.40 s, 5H, Cp). ^{13}C-NMR (ppm): 227.7 (s, CO), 87.6 (d, $^1J_{CH} = 180$ Hz, Cp), 86.6 (d, $^1J_{CH} = 177$ Hz, Cp). Anal. Calc. for $C_{15}H_{10}O_5CrRu$ (FW = 423.30): C, 38.56; H, 2.16%. No further fraction is collected.

4.8. $Cp(CO)_3W–Ru(CO)_2Cp$ (7)

As described above, 523 mg (1.5 mmol) $CpRu(CO)_2I$ in 8 ml THF were reacted with 534 mg (1.5 mmol) $NaW(CO)_3Cp$ in 15 ml THF and kept under reflux for 7 days before standard workup. Fraction 1 (hexane–THF 10:1): mixture of $Cp(CO)_3WH$, $Cp(CO)_3W–Ru(CO)_2Cp$ (**7**) and $Cp(CO)_3W–W(CO)_3Cp$. After removing the solvent the red residue is extracted with cold hexane (2×10 ml) and the combined yellow hexane solutions are freed from the solvent at high vacuum to yield 16 mg (0.05 mmol, 3%) $Cp(CO)_3WH$ (FW = 333.97) as a yellow solid. Fractionized crystallization of the red residue from hexane–THF (10:1) at −40°C yields 207 mg (0.37 mmol, 25%) $Cp(CO)_3W–Ru(CO)_2Cp$ (**7**) as red–orange crystals. Crystals suitable for X-ray crystallography were obtained by recrystallization of **7** from hexane at −40°C. ^{1}H-NMR (ppm): 4.81 (s, 5H, WCp), 4.64 s, 5H, MoCp). ^{13}C-NMR (ppm): 212.1 (s, CO), 88.1 (d, $^1J_{CH} = 179$ Hz, WCp), 87.6 (d, $^1J_{CH} = 180$ Hz, RuCp). Anal. Calc. for $C_{15}H_{10}O_5WRu$ (FW = 555.15): C, 32.45; H, 1.82. Found: C, 33.33; H, 1.91%. The second compound obtained by the fractionised crystallization from hexane–THF, a red solid, is identified as 110 mg (0.17 mmol, 22%) $Cp(CO)_3W–W(CO)_3Cp$ (FW = 665.93). Fraction 2 (hexane–THF 10:1): 88 mg (0.20 mmol, 27%) $[Ru(CO)_2Cp]_2$ (**9**) (FW: 444.4), yellow–orange solid. Fraction 3 (THF): 162 mg (0.46 mmol, 31%) $CpRu(CO)_2I$.

4.9. $[CpRu(CO)_2]_2$ (9)

Yellow rhombs of **9** suitable for X-ray crystallography were obtained from crystallization from hexane at −25°C.

4.10. Attempted synthesis of $Cp(CO)_3Mo–Ru(CO)_3(\eta^3\text{-}C_3H_5)$ (14)

At r.t., a solution of 134 mg (0.5 mmol) $NaMo(CO)_3Cp$ in 5 ml THF, was added dropwise to a suspension of 177 mg (0.5 mmol) of (η^3-C_3H_5)–$Ru(CO)_2I$ in 15 ml THF. The iodide seems to be consumed already after 5 min. The resulting dark red, clear solution was stirred for another 2 days and darkens during the course of the reaction. Column chromatography yielded the four fractions of $[CpMo(CO)_3]_2$ (**8**), $[CpRu(CO)_2]_2$ (**9**), $CpMo(CO)_3I$, $CpRu(CO)_2I$, respectively. Change of parameters (temperature, use of (η^3-C_3H_5)–$Ru(CO)_2Br$, reaction time) did not give rise to the desired product **14**.

4.11. Reactivity studies of $Cp(CO)_3Mo–Ru(CO)_2Cp$ (1)

4.11.1. PPh_3

A solution of 94 mg (0.2 mmol) of $Cp(CO)_3Mo–Ru(CO)_2Cp$ (**1**) and 52 mg (0.2 mmol) PPh_3 in 15 ml THF was stirred for 28 days and then refluxed for 1400 min (24 h). There was no change in the IR spectra.

4.11.2. CS_2

A solution of 185 mg (0.4 mmol) of $Cp(CO)_3Mo–Ru(CO)_2Cp$ (**1**) and 31 mg CS_2 (0.4 mmol) PPh_3 in 20 ml THF was refluxed for 7 days and no change in the IR spectra was detected.

4.11.3. CO_2

A solution of 94 mg (0.2 mmol) of $Cp(CO)_3Mo–Ru(CO)_2Cp$ (**1**) in 15 ml hexane was stirred under CO_2-atmosphere at r.t. for 3 days and no reaction could be detected.

4.11.4. CO

A solution of 94 mg (0.2 mmol) of $Cp(CO)_3Mo–Ru(CO)_2Cp$ (**1**) in 15 ml hexane was stirred under CO-atmosphere at r.t. for 3 days and no reaction could be detected.

4.11.5. $Na(Ph_2CO)$

A solution of 94 mg (0.2 mmol) of $Cp(CO)_3Mo–Ru(CO)_2Cp$ (**1**) in 10 ml THF was stirred vigorously and titrated with a deep blue solution of $Na(Ph_2CO)$ in THF. The quantitative formation of $Na[MoCp(CO)_3]$ (**a**) and $Na[Ru(CO)_2Cp]$ (**b**) was detected. IR (THF) (cm^{-1}): 1901 (vs, **a**, **b**), 1823 (m, **b**), 1796 (s, **a**), 1747 (s, **a**). Upon addition of more $Na(Ph_2CO)$ no further change of the IR spectra was observed.

4.11.6. $K(Ph_2CO)$

A solution of 94 mg (0.2 mmol) of $Cp(CO)_3Mo–Ru(CO)_2Cp$ (**1**) in 10 ml THF was vigorously stirred and titrated with a deep blue solution of $K(Ph_2CO)$ in THF. The quantitative formation of $K[MoCp(CO)_3]$ (**a**) and $K[Ru(CO)_2Cp]$ (**b**) was detected. IR (THF) (cm^{-1}): 1898 (vs, **a**, **b**), 1811 (m, **b**), 1790 (s, **a**), 1750 (s, **a**). Upon addition of more $K(Ph_2CO)$ no further change of the IR spectra was observed.

4.11.7. Br_2

A solution of 94 mg (0.2 mmol) of $Cp(CO)_3Mo–Ru(CO)_2Cp$ (**1**) in 20 ml THF is titrated with a solution of Br_2 in THF until the formation of $CpRu(CO)_2Br$ (**a**) and $CpMo(CO)_3Br$ (**b**) is complete (IR control). IR (hexane) (cm^{-1}): 2054 (vs, **a**, **b**), 2009 (s, **a**), 1984 (vs, **b**), 1963 (m, **b**). IR (THF) (cm^{-1}): 2047 (s, **a**, **b**), 1993 (s, **a**), 1969 (vs, **b**).

4.11.8. I_2

A solution of 94 mg (0.2 mmol) of $Cp(CO)_3Mo$–$Ru(CO)_2Cp$ (**1**) in 20 ml THF is titrated with a solution of I_2 in THF until quantitative formation of $CpRu(CO)_2I$ (**a**) and $CpMo(CO)_3I$ (**b**). IR (THF) (cm^{-1}): 2040 (s, **a**, **b**), 1991 (s, **a**), 1963 (vs, **b**).

4.11.9. $AlCl_3$

Freshly sublimed $AlCl_3$, 533 mg (0.4 mmol), were added to a solution of 94 mg (0.2 mmol) of $Cp(CO)_3$-Mo–$Ru(CO)_2Cp$ (**1**) in 20 ml THF and refluxed for 24 h. $CpRu(CO)_2Cl$ (**a**) and $CpMo(CO)_3Cl$ (**b**) were formed quantitatively with some decomposition of the latter. IR (THF) (cm^{-1}): 2047 (s, **a**, **b**), 1994 (vs, **a**), 1952 (m, **b**).

4.12. X-ray crystallography

Single crystals of the air sensitive compounds were measured in perfluoro polyether RS 3000 (Riedel-de Haën). X-ray diffraction data were collected at 120 K with a Nonius Kappa CCD diffractometer using Mo–K_α radiation ($\lambda = 0.71073$ Å) and ϕ-scan data collection mode with a COLLECT [41] collection program. DENZO and SCALEPACK [42] programs were used for cell refinements and data reduction. All structures were solved by direct methods using SHELXS-97 [43] or SIR-97 [44] programs with the WINGX [45] graphical user interface. A semi-empirical multi-scan absorption correction, based on equivalent reflections (XPREP in SHELXTL version 5.1) [46] was applied to $Cp(CO)_3W$–$Ru(CO)_2Cp$ (**7**) ($T_{max}/T_{min} = 0.4823/0.1839$). All structure refinements were carried out with the SHELXL-97 program [47]. All non-hydrogen atoms were refined anisotropically. For compounds $Cp(CO)_3Mo$–$Ru(CO)_2Cp$* (**2**) and $Cp(CO)_3W$–$Ru(CO)_2Cp$ (**7**) the hydrogens were constrained to ride on their parent atom (C–H = 0.95 Å and $U_{iso} = 1.2$ (C_{eq}) for aromatic hydrogens and C–H = 0.98 Å and $U_{iso} = 1.5$ (C_{eq}) for methyl hydrogens). For compounds $Cp(CO)_3Mo$–$Ru(CO)_2Cp$ (**1**) and $Cp(CO)_3Cr$–$Ru(CO)_2Cp$ (**6**) hydrogens were located from the difference Fourier map and refined isotropically. Although the crystal structure of compound **9** has been published earlier [48], it was redetermined in the current work (data collection at 120 K in contrast to r.t. in Ref. [48b]). The crystallographic details are available as supporting material and selected bond lengths and angles are given in Table 2 for ease of comparison. Crystallographic data of **1**, **2**, **6** and **7** are summarized in Table 1 and selected bond lengths and angles are given in Table 2. The structures and the numbering schemes for complexes $Cp(CO)_3Mo$–$Ru(CO)_2Cp$ (**1**) and $Cp(CO)_3Mo$–$Ru(CO)_2Cp$* (**2**) are presented in Figs. 1 and 2.

5. Supplementary material

Crystallographic data for the structural analysis have been deposited with the Cambridge Crystallographic Data Centre, CCDC 142814 for **1**, 142816 for **2**, 142815 for **6**, 142813 for **7**, 142817 for **9**. Copies of this information may be obtained free of charge from: The Director, CCDC, 12 Union Road, Cambridge, CB2 1EZ, UK (fax: +44-1223-336033; e-mail: deposit@ccdc.cam.ac.uk or www: http://www.ccdc.cam.ac.uk).

Acknowledgements

Funding of this project by the European Union under the TMR Programme, contract ERBFM-RXCT960091, is gratefully acknowledged.

References

[1] M. Rakowski Dubois, M.C. van Derveer, D.L. Dubois, R.C. Haltiwanger, W.K. Miller, J. Am. Chem. Soc. 102 (1980) 7456.
[2] (a) F.E. Masoth, Adv. Catal. 27 (1978) 265. (b) B.C. Wiegand, C.M. Friend, Chem. Rev. 92 (1992) 491
[3] M. Rakowski Dubois, Chem. Rev. 89 (1989) 1 and references therein.
[4] M.J. Morris, in: G. Wilkinson, F.G.A. Stone, E.W. Abel (Eds.), Comprehensive Organometallic Chemistry II, vol. 5, Pergamon, Oxford, 1995 (Chapter 3).
[5] (a) M.D. Curtis, J.E. Penner-Hahn, J. Schwank, O. Baraldt, D.J. McCabe, L. Thomson, G Waldo, Polyhedron 7 (1988) 2411. (b) U. Riaz, O.J. Curnow, M.D. Curtis, J. Am. Chem. Soc. 116 (1994) 4357.
[6] (a) H. Adams, L.J. Gill, M.J. Morris, Organometallics 15 (1996) 464. (b) H. Adams, L.J. Gill, M.J. Morris, Organometallics 15 (1996) 4182. (c) H. Adams, N.A. Bailey, S.R. Gay, T. Hamilton, M.J. Morris, J. Organomet. Chem. 493 (1995) C25. (d) H. Adams, N.A. Bailey S.R. Gay, L.J. Gill, T. Hamilton, M.J. Morris, J. Chem. Soc. Dalton Trans. (1996) 2403. (e) H. Adams, N.A. Bailey A.P. Bisson, M.J. Morris, J. Organomet. Chem. 444 (1993) C34.
[7] M. Cazanoue, L. Noël, J.J. Bonnet, R. Mathieu, Organometallics 7 (1988) 2480.
[8] (a) D.-K. Hwang, Y.B. Chi, S.-M. Peng, G.-H. Lee Organometallics 9 (1990) 2709. (b) D.-K. Hwang, Y.B. Chi, S.-M. Peng, G.-H. Lee J. Organomet. Chem. 389 (1990) C7.
[9] Y. Mizobe, M. Hosomizu, Y. Kubota, M. Hidai, J. Organomet. Chem. 507 (1996) 179.
[10] (a) R.D. Adams, J.E. Babin, M. Tasi, Organometallics 7 (1988) 219. (b) R.D. Adams, J.E. Babin, M. Tasi, J. Inorg. Chem. 25 (1986) 4514.
[11] (a) W. Bernhardt, H. Vahrenkamp, J. Organomet. Chem. 355 (1988) 427. (b) R. Eckehart, W. Bernhardt, H. Vahrenkamp, Chem. Ber. 118 (1985) 2858. (c) T. Albiez, W. Bernhardt, C. von Schnering, R. Eckehart, H. Bantel, H. Vahrenkamp, Chem. Ber. 120 (1987) 141.
[12] (a) D.A. Roberts, G.L. Geoffroy, in: G. Wilkinson, F.G.A. Stone, E.W. Abel (Eds.), Comprehensive Organometallic Chemistry, vol. 6, Pergamon Press, Oxford, 1982 (Chapter 40). (b) Y. Chi, D.-K. Hwang, in: G. Wilkinson, F.G.A. Stone, E.W. Abel (Eds.), Comprehensive Organometallic Chemistry II, vol. 10, Pergamon, Oxford, 1995 (Chapter 3).

[13] M.J. Chetcuti, in: G. Wilkinson, F.G.A. Stone, E.W. Abel (Eds.), Comprehensive Organometallic Chemistry II, vol. 10, Pergamon, Oxford, 1995 (Chapter 2).
[14] J.S. Drage, M. Tilset, K.P.C. Vollhardt, T.W. Weidman, Organometallics 3 (1984) 812.
[15] R. Boese, M.A. Huffman, K.P.C. Vollhart, Angew. Chem. Int. Ed. Engl. 30 (1991) 1463.
[16] B. Chaudret, F. Dahan, S. Sabo, Organometallics 4 (1985) 1490.
[17] R.L. Beddoes, E.S. Davies, M. Helliwell, M.W. Whiteley, J. Organomet. Chem. 421 (1991) 285.
[18] M.L. Ziegler, H.E. Sasse, B. Nuber, Z. Naturforsch. Teil B 30 (1975) 26.
[19] S.A.R. Knox, J. Organomet. Chem. 400 (1990) 255.
[20] J.P. Collman, S.T. Harford, P. Maldivi, J.-C. Marchon, J. Am. Chem. Soc. 120 (1998) 7999.
[21] T. Straub, M. Haukka, T.A. Pakkanen, thirteenth FECHEM, Conference on Organometallic Chemistry, 1999, p. 260.
[22] T. Madach, V. Vahrenkamp, Chem. Ber. 113 (1979) 2675.
[23] C.P. Casey, M.W. Meszaros, R.E. Colborn, D.M. Roddick, W.H. Miles, M. Gohdes, Organometallics 5 (1986) 1879.
[24] J.R. Moss, M.L. Niven, P.M. Strecht, Inorg. Chim. Acta 119 (1986) 177.
[25] R.B. King, A. Efraty, W.M. Douglas, J. Organomet. Chem. 60 (1973) 125.
[26] R. Poli, J.C. Gordon, J.U. Desai, A.L. Rheingold, J. Chem. Soc. Chem. Comm. (1991) 1518.
[27] S.P. Nolan, R. López de la Vega, C.D. Hoff, J. Organomet. Chem. 315 (1986) 187.
[28] A.C. Filippou, W. Grünleitner, E. Herdtweck, J. Organomet. Chem. 373 (1989) 325.
[29] T. Piper, G. Wilkinson, J. Inorg. Nucl. Chem. 3 (1956) 104.
[30] W.A. Herrmann, J. Rohrmann, E. Herdtweck, C. Hecht, M.L. Ziegler, O. Serhaldi, J. Organomet. Chem. 314 (1986) 295.
[31] C. Caballero, F. Oberdorfer, E. Guggolz, B. Nuber, R.P. Korswagen, M.L. Ziegler, Bol. Soc. Quim. Peru 53 (1987) 135 CA, 110, 213022k.
[32] R.D. Adams, D.M. Collins, F.A. Cotton, Inorg. Chem. 5 (1974) 1086.
[33] W. Clegg, N.A. Neville, R.J. Errington, N.C. Norman, Acta Crystallogr. Sect. C 44 (1988) 568.
[34] R.O. Gould, J. Barker, M. Kilner, Acta Crystallogr. Sect. C 44 (1988) 461.
[35] C. Elschenbroich, A. Salzer, Organometallics, A Concise Introduction, second ed., VCH, Weinheim, 1992, p. 229.
[36] T.J. Jaeger, M.C. Baird, Organometallics 7 (1988) 2074.
[37] J.C.T.R. Burckett-St. Laurent, J.S. Field, R.J. Haines, M. McMahon, J. Organomet. Chem. 153 (1978) C19.
[38] D.H. Gibson, W.-L. Hsu, A.L. Steinmetz, B.V. Johnson, J. Organomet. Chem. 208 (1981) 89.
[39] H. Nagashima, K. Mukai, Y. Shiota, K. Yamaguchi, K. Ara, T. Fukahori, H. Suzuki, M. Akita, Y. Moro-oka, K. Itoh, Organometallics 9 (1990) 799.
[40] G. Sbrana, G. Braca, F. Piacenti, P. Pino, J. Organomet. Chem. 13 (1968) 240.
[41] COLLECT data collection software, Nonius, 1999.
[42] Z. Otwinowski, W. Minor, Methods in enzymology, in: C.W. Carter, Jr., R.M. Sweet (Eds.), Macromolecular Crystallography, Part A, vol. 276, Academic Press, New York, 1997, p. 307.
[43] G.M. Sheldrick, SHELXS-97, Program for Crystal Structure Determination, University of Göttingen, 1997.
[44] A. Altomare, C. Cascarano, C. Giacovazzo, A. Guagliardi, A.G.G. Moliterni, M.C. Burna, G. Polidori, M. Camalli, R. Spagna, SIR-9, A Package for Crystal Structure Solution by Direct Methods and Refinement, University of Bari, Italy, 1997.
[45] L.J. Farrugia WINGX version 1.61, A Windows Program for Crystal Structure Analysis, University of Glasgow, Glasgow, 1998.
[46] G.M. Sheldrick, SHELXTL version 5.1, Bruker Analytical X-ray Systems, Bruker AXS, Inc., Madison, WI, 1998.
[47] G.M. Sheldrick, G.M. SHELXL-97, Program for Crystal Structure Refinement, University of Göttingen, 1997.
[48] (a) O.S. Mills, J.P. Nice, J. Organomet. Chem. 9 (1967) 339. (b) J.T. Mague, Acta Crystallogr. Sect. C 51 (1995) 831.